Journal of Cardiovascular Magnetic Resonance®, 2(1), 33–41 (2000)

Global Alterations in Mechanical Function in Healed Reperfused First Anterior Myocardial Infarction

Christopher M. Kramer, Charles J. McCreery, Lori Semonik, Walter J. Rogers, Thomas P. Power, Amy Shaffer, and Nathaniel Reichek

Division of Cardiology, Department of Medicine, Allegheny General Hospital, Pittsburgh, Pennsylvania

ABSTRACT

Two-dimensional analysis techniques were applied to breathhold magnetic resonance (MR) tagged images in humans to better understand left ventricular (LV) mechanics 8 weeks after large reperfused first anterior myocardial infarction (MI). Eighteen patients (aged 51 ± 13 yr, 15 men) were studied 8 ± 1 weeks after first anterior MI as were 9 volunteers, (aged 30 ± 3, 7 men). Breathhold MR myocardial tagging was performed with short-axis images spanning the LV from apex to base. Myocardial deformation was analyzed from apical, mid-LV, and basal slices using two-dimensional analytic techniques and expressed as L1 (greatest systolic lengthening), L2 (greatest systolic shortening), and β (angular deviation of L1 from the radial direction). LV ejection fraction (EF) by MR imaging in the patients after MI was 45 ± 15%. The apex and midventricle in patients demonstrated reduced L1 and L2 and increased β compared with normal subjects with the greatest abnormalities at the apex, as expected in anterior infarction. However, in addition, basal L1 was lower than normal subjects (10 ± 6% versus 19 ± 7%, $p < 0.0001$) as was L2 (14 ± 7% versus 17 ± 6%, $p < 0.04$). β was greater than normal at the base (23 ± 20 degrees and 14 ± 10 degrees, $p < 0.02$). L2 correlated significantly with EF in the patient group ($EF = 2.6 \times L2 + 7$, $r = 0.68$, $p < 0.002$). After healing of reperfused first anterior MI, maximal lengthening and maximal shortening and the orientation of maximal strains are abnormal throughout the left ventricle, including mild abnormalities at the base. This suggests more diffuse abnormalities in regional mechanical function than simply within the zone of healed infarction.

KEY WORDS: *Magnetic resonance imaging; Mechanics; Myocardial contraction; Myocardial infarction.*

Received March 25, 1999; Accepted August 25, 1999

Address correspondence to Christopher M. Kramer, University of Virginia Health System, Depts. of Medicine and Radiology, Box 170, Charlottesville, VA 22908.

INTRODUCTION

Previous methods used to evaluate myocardial function after myocardial infarction (MI) track endocardial motion (1) or wall thickening (2). These methods are limited in infarcted myocardium by passive motion due to pull from dyskinetic and/or normal regions and by motion of the heart through the imaging plane. Measurements of strains in two and three dimensions have been performed with invasive marker implantation but may be limited by myocardial damage caused by the implants and the small number of sites sampled (3–5). Magnetic resonance (MR) myocardial tagging (6,7) allows one- (1D) (8), two- (2D) (9), and three-dimensional (10) analysis of intramyocardial motion and deformation. Tag stripe intersections can be used to delineate planar triangular myocardial elements and assess their deformation during systole. Assuming homogenous strain within each triangle, the deformation of the triangles can be calculated (9). Using MR tagging in an animal model of chronic infarction, we previously demonstrated abnormal mechanical function in infarcted and adjacent noninfarcted myocardium using 1D (11) and 2D analyses (12). In 1D analysis of tagged images in humans, we demonstrated abnormal circumferential shortening in remote noninfarcted myocardium early after anterior MI (13) that later improved to some extent (14). Others have used 2D analysis techniques early after anterior MI (15). To better understand myocardial mechanical function in healed human infarction, we applied 2D analysis techniques to MR tagged images in humans 8 weeks after large reperfused first anterior MI.

MATERIALS AND METHODS

Patient Population

The study was approved by the Institutional Review Committee in accordance with institutional guidelines. All gave informed consent. Eighteen patients, 15 men, aged 51 ± 13 yr, were studied 8 ± 1 weeks after first anterior MI. All had an initially occluded left anterior descending (LAD) artery and no other arteries with a >50% stenosis and had been treated acutely with thrombolytics ($n = 3$), primary angioplasty ($n = 11$), or thrombolysis followed by rescue angioplasty ($n = 4$). The mean time to the start of reperfusion therapy was 388 ± 210 min in the 16 patients for whom this was known. The peak creatine kinase was 3167 ± 2190. All had a patent infarct-related artery and TIMI III flow by contrast angiography in the first several days after infarction. The mean ejection fraction (EF) by left ventriculography or echocardiography in the first week post-MI was 40 ± 8%. The patients' medications during the 8-week period after infarction included aspirin in 15, angiotensin-converting enzyme inhibitors in 15, beta-blockers in 13, warfarin in 8, digoxin in 4, nitrates in 2, and diuretics in 1.

Nine volunteers with normal echocardiograms at baseline were studied with the same techniques; seven were men and their mean age 30 ± 3 yr.

MR Imaging

MR imaging was performed in a Siemens Magnetom SP 1.5-T scanner with the patient prone on an elliptical spine surface coil. The imaging protocol was well described previously (13,14). Briefly, localizing scout images were followed by a short-axis cine series in a plane near the mitral valve, which provided images every 40 msec to identify end-systole as the point of minimum left ventricular (LV) cavity area. A series of multiphase, short-axis, single-slice, tagged images were obtained using a breathhold multiple phase-encoded gradient-echo method and segmented k-space trajectory. Tag stripe separation was 7 mm, field of view was 280 mm, and matrix size 128 × 256, interpolated to 256 × 256 for display, yielding a pixel size of 1.19 mm^2. Image planes 7 mm thick were generated, spanning the entire LV cavity from apex to base (Fig. 1). The breathhold spanned 18 heartbeats or 14–15 sec per breathhold. TR (repetition time) was adjusted (from a minimum of 58 msec to a maximum of 90 msec) so as to time one image during the five-phase image series at end-systole.

Image Analysis

Regional function was analyzed using a software package (SPAMMVU, © Univ. of PA) loaded on a Silicon Graphics workstation and previously published methods (9,12,15). The epicardial and endocardial contours of the left ventricle were manually traced at each phase of the cardiac cycle in three slices, one each from apex, midventricle, and base. Tag stripes were then tracked through systole using an automated tracking procedure based on an active contour model. Triplets of stripe intersections defined triangular elements within the myocardium (Fig. 2). Most of these triangles were midmyocardial due to the 7-mm interstripe distance with a wall thickness of 10–12 mm. Within each element, components of systolic deformation of the triangle were measured, including L1 (greatest systolic stretch or percent-

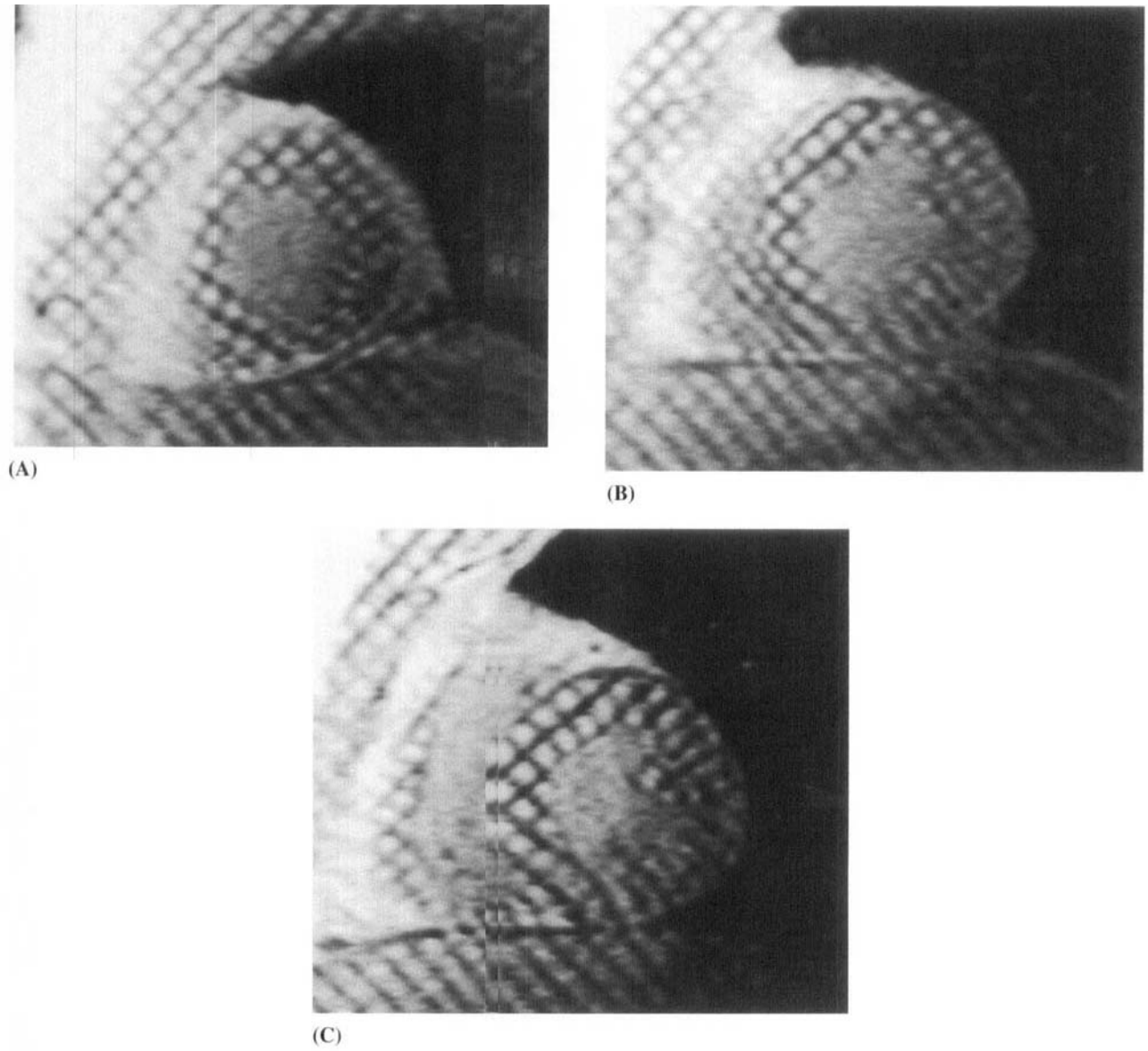

Figure 1. (A) End-systolic breathhold gradient-echo MR tagged image at the apex in a patient 8 weeks after anterior MI treated with primary angioplasty. The intraventricular septum lies from 7 o'clock to 10 o'clock on the image adjacent to the right ventricle (RV) apex, the anterior wall from 10 o'clock to 1 o'clock, the lateral free wall from 1 o'clock to 4 o'clock, and the inferior wall from 4 o'clock to 7 o'clock. Note the thinning of the anterior septum and the reduced deformation of the tag stripes around the entire circumference of the left ventricle. (B) End-systolic breathhold gradient-echo MR tagged image at the midventricle in the same patient and same orientation with the intraventricular septum and mid RV seen from 7 o'clock to 10 o'clock on the image. Deformation of the tag stripes is better preserved in the lateral and inferior walls. (C) End-systolic breathhold gradient-echo MR tagged image at the base in the same patient and same orientation with the intraventricular septum and RV outflow tract seen from 7 o'clock to 11 o'clock on the image. The anterior wall and septum demonstrate normal wall thickness but reduced deformation.

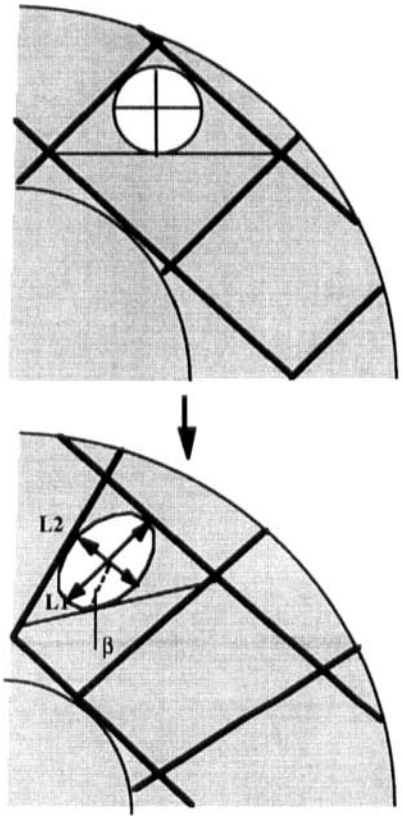

Figure 2. Schematic representation of the strain analysis at end-diastole (top) and end-systole (bottom) in a single triangle within the wall of the LV. The triangle has deformed at end-systole with L1 = greatest systolic lengthening, L2 = greatest systolic shortening, β = angular deviation of L1 from the radial direction.

age of systolic lengthening in the direction of maximum lengthening), L2 (greatest systolic shortening or percentage of shortening in the direction of greatest shortening), and β (angular deviation of L1 from the radial direction) (9,12,15).

LV mass was calculated from planimetered epicardial and endocardial areas of stacked short-axis end-diastolic tagged images from apex to base using Simpson's rule according to previously published techniques (11,14) and was indexed to body surface area. LV end-diastolic volume index, LV end-systolic volume index, and EF were calculated using planimetered end-diastolic and end-systolic areas in the same manner.

Statistical Analysis

Comparisons between patients and normal subjects were made using Student's *t*-test for unpaired comparisons. Linear regression analysis was performed for EF and end-systolic volume index versus L1, L2, and β, respectively. Results are displayed as mean ± SD. $p < 0.05$ was considered significant.

RESULTS

Global LV Parameters

During the MR scan, the patients' heart rate was 74 ± 15, systolic blood pressure 122 ± 21, and diastolic blood pressure 74 ± 17. Analysis of the MR images demonstrated that the LV mass index was 102 ± 19 g/m^2, the LV end diastolic volume index was 101 ± 28 ml/m^2, and the end-systolic volume index was 56 ± 25 ml/m^2. The EF was 45 ± 15%.

Maximum Principal Strain

At the apex, all regions around the short axis demonstrated depressed L1 compared with normals, save for the lateral wall (Table 1). When the results from all four regions were averaged, the apex in patients had an L1 of 5 ± 13% versus 15 ± 5% in normal subjects ($p < 0.0001$). Similarly, in the midventricle, only the lateral wall demonstrated normal L1. The midventricle as a whole had a lower L1 than normal (8 ± 7% versus 15 ± 5%, $p < 0.0001$). At the base, all four regions around the LV base showed depressed L1, and when averaged the basal L1 was significantly lower than normals (10 ± 6% versus 19 ± 7%, $p < 0.0001$).

When levels along the long axis were averaged, all four circumferential regions demonstrated reduced L1 when compared with volunteers. The septum had a L1 of 6 ± 15% compared with 19 ± 7% in normals ($p < 0.0001$). Anterior L1 was 6 ± 6% versus 13 ± 5% in normals ($p < 0.0001$), and in the lateral wall L1 was 12 ± 7% compared with 18 ± 6% ($p = 0.0003$). In the inferior wall, L1 was 7 ± 6% in the MI patients and 15 ± 5% in normal subjects ($p < 0.0001$).

Minimum Principal Strain

All regions around the LV short axis at the apex had decreased minimum principal strain (Table 2) and the apex as a whole had an L2 of 14 ± 8% compared with 23 ± 5% for normals ($p < 0.0001$). Similarly, all regions in the midventricle showed decreased L2 and on average had an L2 of 15 ± 7% versus 21 ± 5% in human volunteers ($p < 0.0001$). At the base, only the septum demonstrated a decrease in L2 (11 ± 6% in patients compared with 17 ± 3% in normals, $p < 0.0001$), but the base as

Table 1

L1 in the Two Groups

	Septum	Anterior	Lateral	Inferior	Average
Apex					
Normals	19 ± 6	12 ± 5	18 ± 6	14 ± 5	15 ± 5
AMI	0 ± 5*	6 ± 4†	10 ± 8	4 ± 7†	5 ± 13‡
Midventricle					
Normals	16 ± 4	11 ± 5	17 ± 6	14 ± 4	15 ± 5
AMI	8 ± 7§	6 ± 7*	13 ± 6	8 ± 5§	8 ± 7‡
Base					
Normals	22 ± 8	15 ± 6	21 ± 6	16 ± 6	19 ± 7
AMI	10 ± 7†	8 ± 6*	12 ± 6§	8 ± 5§	10 ± 6‡
Average					
Normals	19 ± 7	13 ± 5	18 ± 6	15 ± 5	
AMI	6 ± 15‡	6 ± 6‡	12 ± 7†	7 ± 6‡	

* $p < 0.05$ vs. normal subjects.
† $p < 0.0001$ vs. normal subjects.
‡ $p < 0.001$ vs. normal subjects.
§ $p < 0.01$ vs. normal subjects.
AMI, acute myocardial infarction.

a whole had significantly decreased L2 at 14 ± 7% versus 17 ± 6% in normal subjects ($p < 0.04$).

When data across the LV long-axis levels were averaged, L2 was decreased in each region around the short axis. Septal L2 was reduced (11 ± 6% compared with 17 ± 3%, $p < 0.0001$) as was anterior L2 at 16 ± 8% (versus 22 ± 5% in normals, $p = 0.0002$). Lateral L2 was 17 ± 6% in patients and 24 ± 5% in volunteers ($p < 0.0001$), and inferior L2 was similarly decreased (14 ± 7% compared with 19 ± 7%, $p < 0.01$).

Angle of Maximum Principal Strain

The relationship of maximum principal strain to the radial direction is altered after anterior MI, greatest in the apex (Table 3). β is greater in patients than in normal

Table 2

L2 in the Two Groups

	Septum	Anterior	Lateral	Inferior	Average
Apex					
Normals	20 ± 3	25 ± 4	25 ± 8	24 ± 6	23 ± 5
AMI	12 ± 8*	15 ± 9*	16 ± 7†	15 ± 7†	14 ± 8‡
Midventricle					
Normals	16 ± 2	22 ± 4	27 ± 3	19 ± 4	21 ± 5
AMI	11 ± 4§	16 ± 7‡	19 ± 7†	15 ± 5§	15 ± 7‡
Base					
Normals	16 ± 4	20 ± 5	21 ± 5	14 ± 7	17 ± 6
AMI	10 ± 4*	18 ± 7	17 ± 5	13 ± 7	14 ± 7§
Average					
Normals	17 ± 3	22 ± 5	24 ± 5	19 ± 7	
AMI	11 ± 6‡	16 ± 8†	17 ± 6‡	14 ± 7*	

* $p < 0.01$ vs. normal subjects.
† $p < 0.001$ vs. normal subjects.
‡ $p < 0.0001$ vs. normal subjects.
§ $p < 0.05$ vs. normal subjects.
AMI, acute myocardial infarction.

Table 3

β (in Degrees) in the Two Groups

	Septum	Anterior	Lateral	Inferior	Average
Apex					
Normals	11 ± 7	18 ± 6	7 ± 4	11 ± 6	12 ± 7
AMI	41 ± 20*	37 ± 21†	30 ± 22‡	28 ± 16‡	34 ± 20§
Midventricle					
Normals	9 ± 2	10 ± 3	6 ± 2	15 ± 10	10 ± 6
AMI	27 ± 19‡	24 ± 19†	17 ± 19	21 ± 12	22 ± 18§
Base					
Normals	9 ± 3	17 ± 7	9 ± 6	21 ± 15	14 ± 10
AMI	21 ± 20	32 ± 24	19 ± 18	19 ± 13	23 ± 20†
Average					
Normals	10 ± 5	15 ± 6	7 ± 4	16 ± 11	
AMI	30 ± 21§	31 ± 22*	22 ± 20*	23 ± 14†	

* $p < 0.001$ vs. normal subjects.
† $p < 0.05$ vs. normal subjects.
‡ $p < 0.01$ vs. normal subjects.
§ $p < 0.0001$ vs. normal subjects.
AMI, acute myocardial infarction.

subjects in all regions around the short axis in the apex and for the apex as a whole is 34 ± 20 degrees compared to 12 ± 7 degrees ($p < 0.0001$). In the midventricle, β is significantly greater than normal in the septum (27 ± 19 compared with 9 ± 2 degrees, $p = 0.01$) and anterior wall (24 ± 19 versus 10 ± 3 degrees, $p < 0.05$) and for the midventricle as a whole (22 ± 19 compared with 10 ± 6 degrees in normal subjects, $p < 0.0001$). At the base, no individual region is abnormal, but on average the base demonstrates a greater β than normal (23 ± 20 and 14 ± 10 degrees, respectively, $p < 0.02$).

When data across the LV long-axis levels were averaged, the angle β was increased in each region around the short axis. Septal β was 30 ± 21 compared with 10 ± 5 degrees ($p < 0.0001$) and anterior β was 31 ± 22 compared with 15 ± 6 degrees ($p < 0.001$). Lateral and inferior similarly showed elevated β (22 ± 20 versus 7 ± 4 degrees, $p < 0.001$, and 23 ± 14 compared with 14 ± 10 degrees, $p < 0.05$, respectively).

Relationship Between Global and Regional Function

For EF and end-systolic volume index, no significant relationship was found with either L1 or β. However, both correlated significantly with L2. The correlation for EF was EF = 2.6 × L2 + 7 ($r = 0.68$, $p < 0.002$) (Fig. 3). For end-systolic volume index, the relationship was

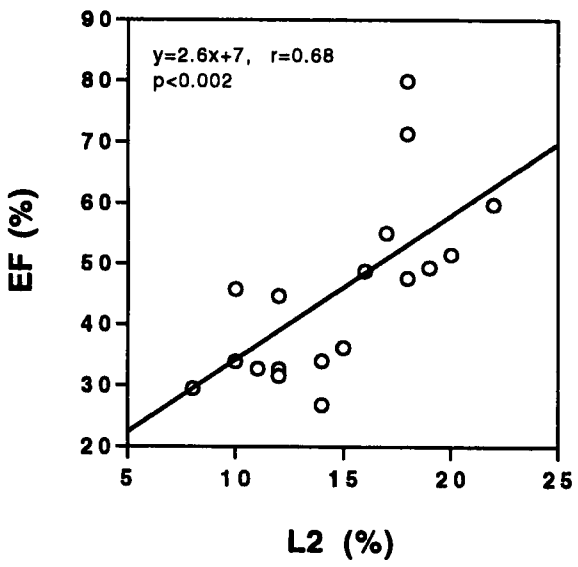

Figure 3. Linear regression analysis of LV EF on the *y* axis versus LV L2 (whole heart) on the *x* axis for each of the patients in the study, demonstrating a significant relationship (EF = 2.6*x*EF + 7, $r = 0.68$, $p < 0.002$).

LV systolic volume index = $125 - 4.6 \times L2$, ($r = 0.74$, $p = 0.0004$).

DISCUSSION

We used MR tagging to noninvasively track myocardial mechanical function through systolic in patients 8 weeks after large anterior MI and single-vessel LAD disease and compared it with a cohort of normal volunteers. We found that after healing of reperfused first anterior MI, the maximum and minimum principal strain and the orientation of maximal strain are abnormal throughout the left ventricle. The abnormalities in deformation are greatest as expected at the apex of the left ventricle. However, the base demonstrates abnormal mechanics, including mildly abnormal maximum and minimum principal strain and abnormal direction of the maximal strain, suggesting more diffuse abnormalities in regional mechanical function than simply within the zone of healed infarction. LV EF and LV systolic volume index, the most powerful predictors of outcome post-MI, correlated best with minimum principal strain.

Comparison with Prior Studies

Holmes et al. (5) characterized the changes in deformation over the first 3 weeks post-MI within transmurally infarcted tissue in a pig model using implanted radiopaque markers. They found significant scar shrinkage and passive deformation due to shearing of the endocardium relative to the epicardium. Wall thickening appeared to be preserved due to this shearing motion but was overestimated due to the passive deformation. They concluded that analysis of wall thickening alone may be an inadequate assessment of intramyocardial function postinfarction. The present study demonstrated that the greatest segment lengthening was not in the direction of wall thickening but was in an oblique direction in the infarcted apex and at the base. In addition, greatest lengthening did not correlate with global EF.

The first MR tagging studies applying 2D analysis of intramyocardial strains in healed infarction were in an ovine model 8 weeks after transmural anteroapical MI (16). Maximal lengthening and maximal shortening were reduced (13 ± 3% and 13 ± 3%, respectively) in the short-axis plane in noninfarcted adjacent regions in comparison with remote regions. These values correspond well to those of the midventricle of the patients in the present study, which likely includes both infarcted and adjacent tissue (8 ± 7% and 15 ± 7%, respectively). In addition, as in the present study, β was abnormal in noninfarcted regions in the ovine model (37 ± 1 degrees in adjacent regions and 20 ± 3 degrees in remote regions).

MR tagging studies of intramyocardial mechanics in human infarction have primarily been performed in the subacute phase. Our previous studies using 1D techniques on day 5 after first anterior MI demonstrated depressed circumferential shortening (%S) throughout the LV, including remote noninfarcted regions (13). Because of abnormal β in these patients, L2 is not directly analagous to %S. In another study using 2D techniques in 10 patients at day 8 after anterior MI (15), the greatest abnormalities in strain parameters were within infarcted regions. By 8 weeks after anterior MI in our 1D analysis (14), %S trended lower at the base (17 ± 3% versus 19 ± 3% in normals, $p = 0.11$), consistent with the findings of the present study. However, %S had improved significantly throughout the LV compared with day 5 post-MI. Extrapolating from the 1D study, 2D strains may be worse in the early postinfarct period than demonstrated at 8 weeks, post-MI in the present study. Preliminary evidence suggests that no further changes in 1D strain occur up to 6 months post-MI (17).

Potential Mechanisms

The change in orientation of the maximum principal strain may be secondary to changes in geometry and fiber alignment in the postinfarct LV as it assumes a more spherical shape (18), causing elevated mechanical load on these regions as estimated in prior studies (19). MacGowan et al. (20) used MR tagging to demonstrate that in the volume overload state of idiopathic dilated cardiomyopathy, shortening in the fiber direction is markedly reduced as is shortening in the cross-fiber direction or 90 degrees to the fiber direction. In the midwall in the human heart, fibers are predominantly circumferential (21). In the present study, the angle of maximum strain is oblique relative to normal, suggesting that the direction of maximal strain is more circumferential, contributing less to wall thickening.

Cell slippage may be another potential cause of the change in orientation of the principal strains (22). Slippage of myocyte bundles may alter fiber orientation and change the direction of maximal strain. Other potential mechanisms include changes in the amount of collagen scar formation (23), although the significance of interstitial collagen within noninfarcted tissue is a matter of some debate (24). Abnormal deformation in noninfarcted myocardium may be caused by stenoses in noninfarct-

related arteries (25), but patients with other than single-vessel LAD disease were excluded from this study.

Limitations

Transmural resolution of the 2D analysis technique is limited due to the 7-mm interstripe distance. Most triangles are therefore in the midwall, and subendocardial and supepicardial mechanics are less well represented. 1D analysis techniques (13) allow improved transmural resolution, as would smaller interstripe distances that are in the developmental stage.

Representative apical, mid, and basal slices were analyzed in the present study. Until more automated analysis techniques are available, the 2D finite element analysis used in this study will not be as easily applied in a multislice fashion that would cover the entire heart.

The control subjects were younger than the patient population, and there may be subtle age-related changes in intramyocardial deformation as shown in a preliminary study by Rademakers et al. (26). This group found in 87 normal volunteers that endocardial fiber shortening fell slightly with age from the second to seventh decade (26.1% to 24.4%, $p < 0.0001$), although epicardial strains remained unchanged with age. The differences in strains in the present study are likely to be greater than could be accounted for by age differences between patients and controls. In addition, controls were normal subjects, as opposed to patients with coronary artery disease without prior infarction. However, intramyocardial strain abnormalities would not be expected at rest in such patients but would be seen more likely under conditions of stress, such as with dobutamine infusion.

Thirteen of the 18 patients were on beta-blockers at the time of study. Beta-blockers have known negative inotropic properties in the acute setting. However, a recent meta-analysis of clinical trials studying chronic beta-blockade in LV dysfunction demonstrated improvement in global systolic function (an increase in EF of 29%) (27).

Future Directions

The advent of MR diffusion imaging will allow study of myofiber orientation in such patients on a local level (28). Combining information about fiber orientation with strain in the future will enhance the understanding of regional myocardial mechanics after infarction. In addition, the ability to noninvasively measure myocardial perfusion with gadolinium-based contrast agents would allow matching of intramyocardial strain patterns with measures of myocardial blood flow (29).

ACKNOWLEDGMENTS

Supported by a grant from the Allegheny Singer Research Institute. We gratefully acknowledge the expertise of the magnetic resonance technologists at Allegheny General Hospital, especially June Yamrozik and Lois Miller.

REFERENCES

1. Martin GV, Sheehan FH, Stadius M, Maynard C, Davis KB, Ritchie JL and Kennedy JW. Intravenous streptokinase for acute myocardial infarction: effects on global and regional systolic function. *Circulation,* 1988; 78:258–266.
2. Jaarsma W, Visser CA, Eenige van MJ, Res JC, Funke Kupper AJ, Verheugt FW and Roos JP. Prognostic implications of regional hyperkinesia and remote asynergy of noninfarcted myocardium. *Am J Cardiol,* 1986; 58:394–398.
3. Waldman LK, Fung Y-C and Covell JW. Transmural myocardial deformation in the canine left ventricle. *Circ Res,* 1985; 57:152–163.
4. Villarreal FL, Waldman LK and Lew WYW. A technique for measuring regional two-dimensional finite strains in canine left ventricle. *Circ Res,* 1988; 62:711–721.
5. Holmes JW, Yamashita H, Waldman LK and Covell JW. Scar remodeling and transmural deformation after infarction in the pig. *Circulation,* 1994; 90:411–420.
6. Zerhouni E, Parrish D, Rogers WJ, Yang A and Shapiro EP. Human heart: tagging with MR imaging—a method for noninvasive measurement of myocardial motion. *Radiology,* 1988; 169:59–64.
7. Axel L and Dougherty L. MR imaging of motion with spatial modulation of magnetization. *Radiology,* 1989; 171:841–845.
8. Clark N, Reichek N, Bergey P, Hoffman EA, Brownson D, Palmon L and Axel L. Normal segmental myocardial function; assessment by magnetic resonance imaging using spatial modulation of magnetization. *Circulation,* 1991; 84:67–74.
9. Young AA, Imai H, Chang C-N and Axel L. Two-dimensional left ventricular deformation during systole using magnetic resonance imaging with spatial modulation of magnetization. *Circulation,* 1994; 89:740–752.
10. Young AA, Kramer CM, Ferrari VA, Axel L, and Reichek N. Three-dimensional deformation in hypertrophic cardiomyopathy. *Circulation,* 1994; 90:854–867.
11. Kramer CM, Lima JAC, Reichek N, Ferrari VA, Llaneras MR, Palmon LC, Yeh I-T, Tallant B and Axel L. Re-

gional function within noninfarcted myocardium during left ventricular remodeling. *Circulation,* 1993; 88:1279–1288.

12. Lima JAC, Ferrari VA, Reichek N, Kramer CM, Palmon L, Llaneras MR, Tallant B, Young AA and Axel L. Segmental motion and deformation of transmurally infarcted myocardium in acute postinfarct period. *Am J Physiol,* 1995; 268:H1304–H1312.
13. Kramer CM, Rogers WJ, Theobald T, Power TP, Petruolo S and Reichek N. Remote noninfarcted region dysfunction soon after first anterior myocardial infarction: a magnetic resonance tagging study. *Circulation,* 1996; 94: 660–666.
14. Kramer CM, Rogers WJ, Theobald TM, Power TP, Geskin G and Reichek N. Dissociation between changes in intramyocardial function and left ventricular volumes in the 8 weeks after first anterior myocardial infarction. *J Am Coll Cardiol,* 1997; 30:1625–1632.
15. Marcus JT, Gotte MJW, van Rossum AC, Kiujer JPA, Heethaar RM, Axel L and Visser CA. Myocardial function in infarcted and remote regions early after infarction in man: assessment by magnetic resonance tagging and strain analysis. *Magn Res Med,* 1997; 38:803–810.
16. Ferrari VA, Kramer CM, Llaneras M, Tallant B, Chang C-N, Reichek N, Axel L and Lima JAC. Mechanical behavior of noninfarcted myocardium adjacent to scarred infarcted tissue during left ventricular remodeling. *Circulation,* 1992; 86:I–679.
17. Kramer CM, Rogers WJ, Theobald TM, Power TP and Reichek N. Left ventricular dilatation progresses despite resolution of remote region dysfunction 6 months after anterior myocardial infarction [abstract]. *Circulation,* 1995; 92:I–316.
18. Mitchell CF, Lamas GA, Vaughan DE and Pfeffer MA. Left ventricular remodeling in the year after first anterior myocardial infarction. *J Am Coll Cardiol,* 1992; 19: 1136–1144.
19. Bogen DK, Rabinowitz SA, Needleman A, McMahon TA and Abelmann WH. An analysis of the mechanical disadvantage of myocardial infarction in the canine left ventricle. *Circ Res,* 1980; 47:728–741.
20. MacGowan GA, Shapiro EP, Azhari H, Siu CO, Hees PS, Hutchins GM, Weiss JL and Rademakers FE. Noninvasive measurement of shortening in the fiber and cross-fiber direction in the normal human left ventricle and in idiopathic dilated cardiomyopathy. *Circulation,* 1997; 96: 535–541.
21. Greenbaum RA, Ho SY, Gibson DG, Becker AE and Anderson RH. Left ventricular fibre architecture in man. *Br Heart J,* 1981; 45:248–263.
22. Weisman HF, Bush DE, Mannisi JA, Weisfeldt ML and Healy B. Cellular mechanisms of myocardial infarct expansion. *Circulation,* 1988; 78:186–201.
23. Uusimaa P, Risteli J, Niemela M, Lumme J, Ikaheimo M, Jounela A and Peuhkurinen K. Collagen scar formation after acute myocardial infarction: relationships to infarct size, left ventricular function and coronary artery patency. *Circulation,* 1997; 96:2565–2572.
24. Marijianowski MMH, Teeling P and Becker AE. Remodeling after myocardial infarction in humans is not associated with interstitial fibrosis of noninfarcted myocardium. *J Am Coll Cardiol,* 1997; 30:76–82.
25. de Albuquerque CP, Kalil-Filho R, Gerstenblith G, Nakano O, Barbosa V, Bellotti G, Pileggi F and Tranchesi B. Long-term function in the remote region after myocardial infarction: importance of significant coronary stenoses in the non-infarct-related artery. *Br Heart J,* 1994; 71:249–253.
26. Rademakers FE, Herregods M-C, Marchal G and Bogaert J. Contradictory effect of aging on left ventricular untwisting and filling [abstract]. *Circulation,* 1996; 94: I-65.
27. Lechat P, Packer M, Chalon S, Cucherat M, Arab T and Boissel JP. Clinical effects of beta-adrenergic blockade in chronic heart failure: a meta-analysis of double-blind, placebo-controlled, randomized trials. *Circulation,* 1998; 98:1184–1191.
28. Reese TG, Weisskoff RM, Smith RN, Rosen BR, Dinsmore RE and Wedeen VJ. Imaging myocardial fiber architecture in vivo with magnetic resonance. *Magn Res Med,* 1995; 34:786–791.
29. Kraitchman DL, Wilke N, Hexeberg E, Jerosch-Herold M, Wang Y, Parrish TB, Chang C-N, Zhang Y, Bache RJ and Axel L. Myocardial perfusion and function in dogs with moderate coronary stenosis. *Magn Res Med,* 1998; 35:771–780.